
# Commutation Torque-ripple Minimization for Brushless DC Motor Based on Quasi-Z-Source Inverter

# Commutation Torque-ripple Minimization for Brushless DC Motor Based on Quasi-Z-Source Inverter

Qian Xun, Yujing Liu
Chalmers University of Technology

***Abstract* – Conventional brushless DC Motor (BLDCM) drive involves a voltage-source inverter with six-step square-wave control, which can be widely used in automated industrial applications. However, high torque ripple due to different current slew rates during the commutation interval would significantly reduce the performance in the high-precision area. To tackle this problem, the paper proposes a novel strategy to reduce the commutation torque-ripple by using a quasi-Z-source inverter. In which, an impedance network is implemented between the power supply and the voltage-source inverter. This could make the equivalent DC-link voltage boosted during the commutation interval to compensate the current dip of commutation phase, and keep incoming and outgoing phase current changing at the same rate. In Matlab/Simulink environment, proposed scheme is developed and simulated. Finally, the effectiveness of the proposed control strategy is validated, the torque ripple can be greatly reduced and with the increased average torque.**

***Index Terms*-- BLDCM, square-wave control, commutation torque-ripple, quasi-Z-inverter, impedance network**

## I. INTRODUCTION

Brushless DC motors (BLDCM), with advantages of simple structure, large starting torque and broad speed regulation, are widely applied in industrial applications of actuators, feed drives, industrial robots, extruder drives [1-2]. However, it still suffers from high commutation torque-ripple caused by six-step square wave control, and this ripple would induce annoying noise and mechanical vibrations [3]. With the advanced requirement of high precision and high reliability of the BLDCM system, analyzing and suppressing commutation torque-ripple have been becoming an essential basis for improving the performance of drive system [4].

Many pieces of research have been performed to analyze and minimize the commutation torque ripple. A detailed analytical study on commutation torque ripple is presented in [5], in which, a conclusion has been drawn that commutation torque-ripple is caused by the different changing rate between shutdown phase current and opening phase current during commutation interval, and it varies with the machine speed. A similar analysis has been conducted in [6], and a strategy based on the criterion of minimizing the error between the commanded torque and the estimated torque has been proposed, it can adjust the phase current to keep a constant output torque and to maintain small ripples.

Many control strategies, such as current feedback regulation [7], overlapping commutation [8], PWM chopper [9], current predictive control [10], torque closed-loop control [11], are proposed to suppress the torque ripple. The current feedback regulation is a method to control the non-commutation phase current and keep it unchanged during the commutation, it achieves a better effect at low speed, but not well at high speed. To achieve good performance at high-speed range, overlapping commutation is generally applied together with PWM method. In the method, the conduction duty ratio is used to separate the low-speed area and high-speed area. PWM chopper is to make the slope rates of incoming and outgoing phase currents match while commutation by optimizing switching state according to the predefined cost function. The same performance is also realized by current predictive control, in which, a predicted current slope and variations by using the estimated back EMF are used to keep the constant torque during commutation region. Also, torque closed-loop control is also one of the control methods to solve the torque ripple problem. This method takes the instantaneous torque as the research object, and the instantaneous torque is regulated directly to suppress the torque ripple.

Among them, improved drive method based on three-phase switches or advanced control algorithm to form a closed loop is usually utilized. However, they still suffer problems of over-compensation and under-compensation, and the effect of the minimization of the torque-ripple might be affected in field-application. Recently, some scholars have proposed the scheme of regulating DC-link voltage by placing a converter in front of the conventional voltage-source inverter. [12] presents a method to suppress the commutation torque ripple by reducing the input voltage based on buck circuit. In [13], super-lift Luo converter is implemented at the input port of the inverter to generate the desired DC input voltage, and this topology is more suitable for high-speed application compared to the method in [12]. A SEPIC converter is introduced in [14] to adjust the DC-link voltage to reduce the commutation torque ripple.

In this paper, a control strategy based on quasi-Z-source (qZSI) inverter is proposed to minimize the commutation torque ripple. To achieve this, an impedance network is implemented in the front of the traditional voltage source inverter. The DC link voltage is regulated by the duty-through state to get the same current slew rates between the shutdown phase and the opening phase. Firstly, the torque

This work was supported in part by Swedish Electromobility Center. The project period is Jan 2017 -Dec 2019.

Qian Xun and Yujing Liu are with the Division of Electric Power Engineering, Department of Electrical Engineering, Chalmers University of Technology, Gothenburg, 41279 Sweden (e-mail: qian.xun@chalmers.se, yujing.liu@chalmers.se).

ripple of BLDCM driven by the six-step square wave is analyzed, and the mathematical model is presented. Followed by this, the commutation torque-ripple and torque-ripple minimization are analyzed. Finally, the validity of the proposed method is proven by simulation.

## II. Torque Ripple Analysis

Generally, the torque-ripple in BLDCM is formed by three categories: cogging torque, reluctance torque and mutual torque. Cogging torque ripple is caused by the interaction between the permanent magnets of the rotor and the stator slots, and this ripple can be reduced through the optimization of the machine design. While reluctance torque ripple is experienced by a ferromagnetic object placed in an external magnetic field, the object is lined up with the external magnetic field. Thus, it can be neglected due to the surface mounted magnets. Due to the interaction of the stator current and the magnetic flux in the rotor, the mutual torque is the main component of the output torque.

When six-step square-wave control is applied in BLDCM, the ideal back EMF waveform, with the trapezoidal wave and flat top part less than 120°, is needed to get the relatively constant output torque. However, due to the existence of the winding inductance, the increase and decrease of the phase current take time and non-commutation phase current also fluctuates during this time, making the actual phase current not the ideal square-wave. The phase current variation will result in the commutation torque ripple, which might reach up to 50% of the average torque.

Therefore, analysis and suppression of commutation torque ripple have become a critical issue in reducing the overall torque ripple in BLDCM.

### A. Mathematical Model

To analyze the mechanism of the commutation torque, the schematic diagram of a typical BLDCM equivalent circuit driven by the conventional three-phase voltage-source inverter is presented as Fig. 1. $V_{in}$ is the input DC-link voltage of the three-phase inverter, and $R_x$ ($x = a, b, c$) is the resistor of phase $x$, $L_x$ ($x = a, b, c$) represents the inductor, and $e_x$ ($x = a, b, c$) is the back EMF.

In Fig. 1, the phase voltage can be described as

$$\begin{bmatrix} v_a \\ v_b \\ v_c \end{bmatrix} = \begin{bmatrix} R & 0 & 0 \\ 0 & R & 0 \\ 0 & 0 & R \end{bmatrix} \begin{bmatrix} i_a \\ i_b \\ i_c \end{bmatrix} + \begin{bmatrix} L & 0 & 0 \\ 0 & L & 0 \\ 0 & 0 & L \end{bmatrix} \begin{bmatrix} \dot{i}_a \\ \dot{i}_b \\ \dot{i}_c \end{bmatrix} + \begin{bmatrix} e_a \\ e_b \\ e_c \end{bmatrix} + \begin{bmatrix} V_{No} \\ V_{No} \\ V_{No} \end{bmatrix} \quad (1)$$

Where, $v_x$ ($x = a, b, c$) is the voltage of phase $x$, $R$ is the phase winding resistance in the stator, $i_x$ ($x = a, b, c$) is the phase current, $L$ is the equivalent inductance of the phase winding. Here, $L = L_s - M$, in which, $L_s$ is the self-inductance and $M$ is the mutual inductance. It is assumed that the magnetic resistance of the magnetic circuit does not vary with the rotor position, and $L$, $M$ are the constant. $V_{No}$ is the potential of the neutral point.

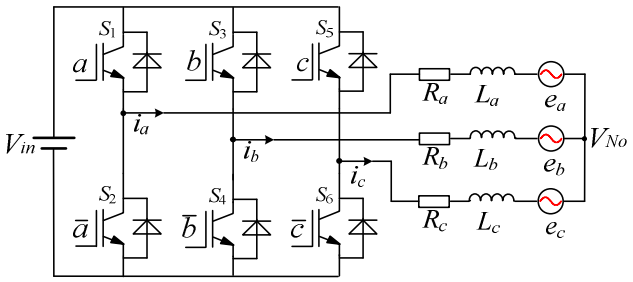


Fig. 1 Schematic diagram of the BLDCM drive system

Without the consideration of cogging torque, the output electromagnetic torque can be expressed as

$$T_e = (e_a i_a + e_b i_b + e_c i_c)\frac{1}{\omega_m} \quad (2)$$

In which, $T_e$ is the electromagnetic torque, and $\omega_m$ is the mechanical angular velocity in the rotor.

Based on the system dynamic principle, mechanical movement equation can be expressed as

$$T_e = J(\frac{d\omega_m}{dt}) + b_m\omega_m + T_l \quad (3)$$

Where $J$ is the system rotational inertia, $b_m$ is the friction coefficient, and $T_l$ is the load torque, which comprises the motor torque generated by no-load losses.

### B. Commutation Torque-ripple

From (2), we can see that the sum of $e_a i_a$, $e_b i_b$ and $e_c i_c$ has to be a constant value to maintain a relatively constant output torque with small ripples. For ideal trapezoidal back EMF, the phase current during one electrical angle period can be shown in Fig. 2.

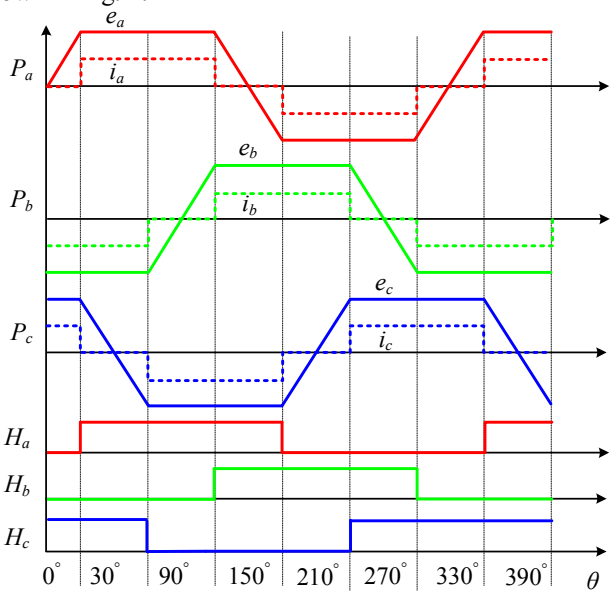


Fig. 2 Ideal current and back EMF with Hall signals

In which, $P_a$, $P_b$, and $P_c$ show the back EMF and phase current, and $H_a$, $H_b$, and $H_c$ represent the corresponding three-phase Hall signals. Since phase winding can be regarded as the inductive load, the phase current cannot increase to a constant value or drop to zero immediately when the commutation starts. It is difficult to achieve the square-wave current during the commutation process, in this time interval, the time difference between the rising current and the falling current will influence the output torque.

Take an example of phase A commuted to phase B, and PWM_ON scheme is adopted to adjust the speed, so phase C is conducted during the commutation.

When neglecting the resistance of the winding, commutation process can be expressed as

$$\begin{cases} L\dfrac{d}{dt}i_a + e_a - L\dfrac{d}{dt}i_c - e_c = 0 \\ L\dfrac{d}{dt}i_b + e_b - L\dfrac{d}{dt}i_c - e_c = V_{in} \end{cases} \tag{4}$$

In the ideal state, $E_a$, $E_b$ and $E_c$ are equal, that is $E_a = E_b = E_c = E$, and for three-phase star-connected BLDCM, it can get the equation of $i_a + i_b + i_c = 0$. By substituting these to (4), we can get

$$\begin{cases} i_a = -\dfrac{V_{in}+2E}{3L}t + I \\ i_b = \dfrac{2(V_{in}-E)}{3L}t \\ i_c = -\dfrac{V_{in}-4E}{3L}t - I \end{cases} \tag{5}$$

Here, $I$ is the current in the steady state during the non-commutation period.

The instantaneous electromagnetic torque during the commutation from phase A to phase B can be expressed as

$$\begin{aligned} T_e &= (e_a i_a + e_b i_b + e_c i_c)\frac{1}{\omega_m} \\ &= (Ei_a + Ei_b + (-E)(-i_a - i_b))\frac{1}{\omega_m} \\ &= -\frac{2Ei_c}{\omega_m} = -K_E i_c \end{aligned} \tag{6}$$

In which, $K_E$ is the coefficient of the back EMF.

Before commutation, the electromagnetic torque is

$$T_0 = \frac{2EI}{\omega_m} \tag{7}$$

When opening phase current reaches to the steady-state value, the electromagnetic torque and torque ripple rate can be expressed as

$$T = \frac{2EI}{\omega_m}(i_a + i_b) = \frac{2EI}{\omega_m}\left[\frac{V_{in}-4E}{2(V_{in}-E)} + 1\right] \tag{8}$$

$$\Delta T = \frac{T - T_0}{T_0} = \frac{V_{in}-4E}{2(V_{in}-E)} \tag{9}$$

The commutation current behaviors in three phases under the different speed ranges can be shown in Fig. 3. From (6), the torque varies linearly with the phase current of non-commutation phase C, it will directly influence the torque ripple. During the commutation, the current of the opening phase B increases, while that of the shutdown phase A decreases, the different changing rates between these result in the current ripple of the non-commutation phase C, thus, the output torque will vary along with the phase C current.

When BLDCM operates at low speed or blocked, then $E \approx 0$, that is $V_{in} > 4E$, we can get the torque ripple is close to 50%, and the phase current is shown as Fig. 3(a). The dropping time ($t_1$) of the shutdown current changing to zero is greater than the rising time ($t_2$) of the opening current changing to a constant value. As shown as Fig. 3(b), when BLDCM operates at high-speed region, we can get $V_{in} \approx 2E$, that is $V_{in} < 4E$, the torque ripple is close to -50% and $t_1$ is smaller than $t_2$. When $V_{in} = 4E$ shown as Fig. 3(c), $t_1$ equals to $t_2$, commutation torque is constant, and there is no torque ripple. Thus, it should be satisfied that $V_{in} = 4E$ in order to get the zero-torque ripple.

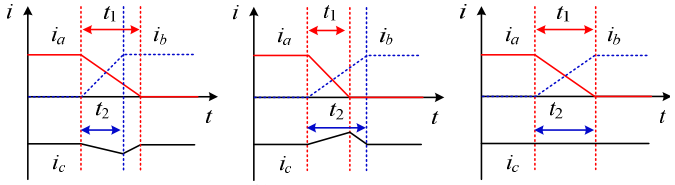


(a) $V_{in} > 4E$, $t_1 > t_2$ (b) $V_{in} < 4E$, $t_1 < t_2$ (c) $V_{in} = 4E$, $t_1 = t_2$

Fig. 3 Commutation current under different speed ranges

## C. Commutation Time

The duty ratio of the PWM at a steady conduction state is $D_0$, while the duty ratio during commutation interval is $D_1$. Take an example of phase A commuted to phase B, when considering the resistance of the winding, the voltage equation during commutation process can be expressed as

$$\begin{cases} Ri_a + L\dfrac{d}{dt}i_a + e_a - Ri_c - L\dfrac{d}{dt}i_c - e_c = 0 \\ Ri_b + L\dfrac{d}{dt}i_b + e_b - Ri_c - L\dfrac{d}{dt}i_c - e_c = V_{in}D_1 \end{cases} \tag{10}$$

The current equation can be described as

$$\begin{cases} \dfrac{di_a}{dt} + \dfrac{i_a}{\tau} = \dfrac{-2E - V_{in} + \dfrac{4E}{T}t}{3R\tau} \\ \dfrac{di_b}{dt} + \dfrac{i_b}{\tau} = \dfrac{-2E + 2V_{in} - \dfrac{2E}{T}t}{3R\tau} \\ \dfrac{di_c}{dt} + \dfrac{i_c}{\tau} = \dfrac{4E - V_{in} - \dfrac{2E}{T}t}{3R\tau} \end{cases} \tag{11}$$

Where, $\tau = L/R$ is the electromagnetic time constant.

According to (10), (11), one can get an approximate expression of phase current

$$\begin{cases} i_a = -\dfrac{2E+V_{in}}{3R} + \dfrac{3RI_0 + 2E + V_{in}}{3R\tau}e^{-t/\tau} \\ i_b = \dfrac{2V_{in}-2E}{3R}\left(1 - e^{-t/\tau}\right) \\ i_c = \dfrac{4E-V_{in}}{3R} - \dfrac{3RI_0 + 4E - V_{in}}{3R}e^{-t/\tau} \end{cases} \tag{12}$$

At time $t_1$, phase A current drops to zero, and the current of phase B and phase C can be described as

$$i_b(t_1) = -i_c(t_1) = \frac{(2V_{in}-2E)I_0}{3RI_0 + V_{in} + 2E} \tag{13}$$

Based on (6), (13), the electromagnetic torque at time $t_1$ can be expressed as

$$T_e = -K_E I_c(t_1) = \frac{K_E(2V_{in}-2E)I_0}{3RI_0 + V_{in} + 2E} \tag{14}$$

The state when phase A/C conducted corresponds to 60°state angle, and the corresponded commutation time can

be expressed as

$$T = \frac{60}{pn} \times \frac{1}{6} = \frac{10}{pn} \tag{15}$$

Where, $p$ is the number of pole pairs, and $n$ is the rotational speed.

The ratio between the commutation period and the electromagnetic time constant can be described as

$$x = \frac{T}{\tau} = \frac{10}{pn\tau} \tag{16}$$

The relationship between the dropping time $t_1$ of the shutdown phase and the commutation time is described as

$$\frac{t_1}{T} = \frac{1}{x}\ln\left(1 + \frac{3}{2}\frac{1-K_u}{1+K_u}\xi\right) \tag{17}$$

Where, $\xi = \frac{2\left(1-e^{-x}\right)}{2-e^{-x}}$. Let $B = \frac{3\left(1-K_u\right)}{1+K_u}$, $K_u = 2E/V_{\rm dc}$ is the speed ratio, then $\frac{t_1}{T} = \frac{1}{x}\ln\left(1+\frac{B}{2}\xi\right)$.

when $x$ is small enough, that is $x \to 0$, $\ln(1+x) \approx x$, and $1\text{-}e^{-x} \approx x$. One can get

$$\begin{aligned} \frac{t_1}{T} &= \frac{1}{x}\ln\left(1+\frac{B}{2}\xi\right) \approx \frac{B}{2x}\xi = \frac{B}{2x}\frac{2\left(1-e^{-x}\right)}{2-e^{-x}} \\ &\approx B \approx \frac{3\left(1-K_u\right)}{\left(1+K_u\right)} \end{aligned} \tag{18}$$

At high-speed region, $K_u = 0.5$, that is $4E = U$, $t_1/T \approx 1$; at medium speed region, $K_u \geq 0.5$, that is $4E \geq U$, $t_1/T \leq 1$, and at the low-speed region, $K_u \leq 0.5$, that is $4E \leq U$, $t_1/T \geq 1$. The analysis results are consistent with the results obtained by ignoring the winding resistance, thus, non-commutation phase current bumps only exist under the condition of large $L$, large time constant and low speed.

When $x$ is big enough, $t_1/T$ tends to 0. Fig. 4 shows the relation between $t_1/T$ and $K_u$, $x$. For most of BLDCM, if $x$ is greater than 0.5, $t_1/T < 0.5$, the case of $t_1 > T$ does not exist. Only when $x$ is relatively small, and at the low-speed region of $K_u < 0.5$, it is possible to have the relation of $t_1 > T$. Therefore, most BLDCM produces positive torque ripple during the commutation interval in an actual situation, which shown as Fig. 3(b).

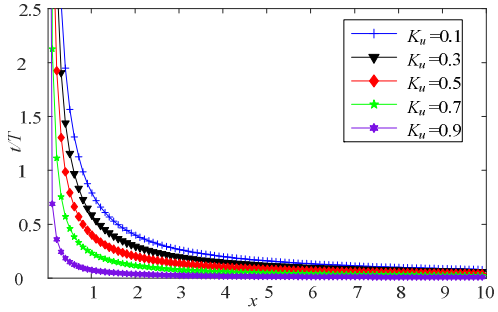


Fig. 4 Trend of $t_1/T$ along with $K_u$ and $x$

## III. Torque Ripple Minimization

The back EMF of the BLDCM is related to its rotational speed, and the higher speed will lead to a bigger back EMF, resulting in a higher voltage requirement. Therefore, the DC-link voltage $V_{in}$ must be increased at high speed to meet the equation of $V_{in} = 4E$; at low speed, $V_{in}$ should be decreased. However, the conventional three-phase voltage-source inverter is a step-down inverter. When BLDCM operates at low speed, it can be controlled by PWM scheme to reduce the DC-link voltage loaded on the motor to suppress the commutation torque ripple, while at high speed, the voltage of the DC-link cannot be raised. To solve the problem and inability to boost the voltage at high speed, the qZSI based on the impedance network is introduced to adjust the dc-link voltage during the commutation.

### A. Quasi-Z-Source Inverter

The topology of qZSI with a continuous current is shown as Fig. 5. It has two general operation states, including the shoot-though state and the non-shoot-though state. In the shoot-though state, the phase leg of the inverter is treated as a short circuit, the switch $S_7$ is open, and the parallel diode is reversely blocked, the voltage can be boosted in this interval. Whereas, in the non-shoot-though state, the phase leg of the inverter is equivalent to a current source viewed from the DC side same as the conventional voltage-source inverter. The equivalent circuits of two states are shown as Fig. 6.

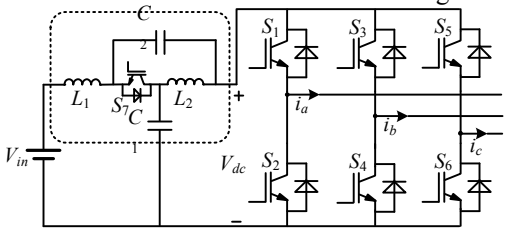


Fig. 5 qZSI with continuous input current

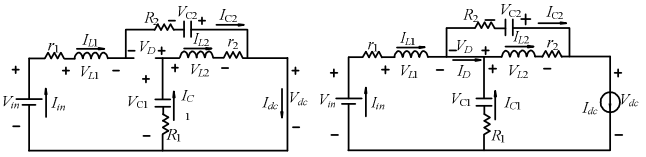


(a) shoot-though state (b) non-shoot-though state

Fig. 6 Equivalent circuit of quasi-Z source inverter

If the interval of the shoot-though state is $T_{\rm sh}$ during one switching cycle $T_{\rm s}$, then the duty ratio of the shoot-though $D = T_{\rm sh}/T_{\rm s}$. From the Fig. 6(a), we have

$$\begin{cases} v_{L1} = V_{C2} + V_{in} \\ v_{L2} = V_{C1} \\ V_{dc} = 0 \end{cases} \tag{19}$$

Where, $v_{\rm L1}$, $v_{\rm L2}$ are the inductor voltage of the impedance network; $V_{\rm C1}$, $V_{\rm C2}$ are the capacitor voltage of the impedance network; and $V_{\rm in}$ is the input voltage of the qZSI.

Fig.6(b) shows the non-shoot-though state, which has the identical working property with the traditional voltage source inverter. During the non-shoot-through interval of ($T_{\rm s}$ - $T_{\rm sh}$), one can get

$$\begin{cases} v_{L1} = V_{in} - V_{C1} \\ v_{L2} = -V_{C2} \\ V_{dc} = V_{C1} - v_{L2} = V_{C1} + V_{C2} \end{cases} \tag{20}$$

In which, $V_{dc}$ is the DC-link voltage of qZSI.

At steady state, the average voltage of the inductor in one switching cycle is zero. According to (19) and (20), we have

$$\begin{cases} D(V_{in}+V_{C2})+(1-D)(V_{in}-V_{C1})=0 \\ DV_{C1}+(1-D)(-V_{C2})=0 \end{cases} \tag{21}$$

Simplify (20), one can get

$$\begin{cases} V_{C1}=\dfrac{1-D}{1-2D}V_{in} \\ V_{C2}=\dfrac{D}{1-2D}V_{in} \\ V_{dc}=\dfrac{1}{1-2D}V_{in}=B_1V_{in} \end{cases} \tag{22}$$

Where, $B_1$ is the boost factor benefited from the shoot-through state.

When $D < 0.5$, we have

$$B=\frac{1}{1-2D}\geq 1 \tag{23}$$

The average output voltage of impedance network is

$$\bar{V}_{dc}=\frac{1-D}{1-2D}V_i \tag{24}$$

The modulation index is $M$, then there is

$$\bar{V}_{dc}=B_1MV_i \tag{25}$$

Where, $B_1M \in (0, +\infty)$, and in theory, the quasi-Z-source network can output arbitrary desired voltage values. When adjusting the DC-link voltage during the commutation period, the commutation current will maintain a constant, and the commutation torque ripple will be minimized.

### B. Control Strategy

From Fig. 3, we can see that the current rate of the shutdown phase and that of the opening phase would be equal to reduce the commutation torque ripple. The following equation should be satisfied

$$\frac{di_a}{dt}=-\frac{di_b}{dt} \tag{26}$$

By substituting (26) to (10), the phase voltage required to produce a constant torque during the commutation interval can be calculated as

$$V_{dc}=3R\left(i_a+i_b\right)+4E-\frac{2E}{T}t \tag{27}$$

By substituting (27) to (13), one can get

$$V_{dc}=3RI+4E_m-\frac{2E_mt}{Te^{-\frac{Rt}{L}}} \tag{28}$$

According to (17), the commutation time can be calculated as

$$t=\frac{L}{R}\ln\left(1+\frac{3RI}{V_{dc}+2E}\right) \tag{29}$$

During the commutation interval, the torque ripple can be reduced by adjusting the voltage to satisfy (28).

Before commutation, the current falling time of the shut-down phase is calculated as the commutation time $t$, it can be obtained by (29), and the real commutation interval $t'$ would be increased when the BLDCM speed changes. To meet this requirement, a small-time interval $\Delta t$ is used to correct $t$, and the real commutation time can be calculated as $t' = t + \Delta t$. The proposed control strategy can be shown as Fig. 7.

Fig. 8 is a schematic diagram for reducing torque ripple, non-commutation current drops during the commutation, while the current tends to ideal trapezoidal wave after the voltage compensation.

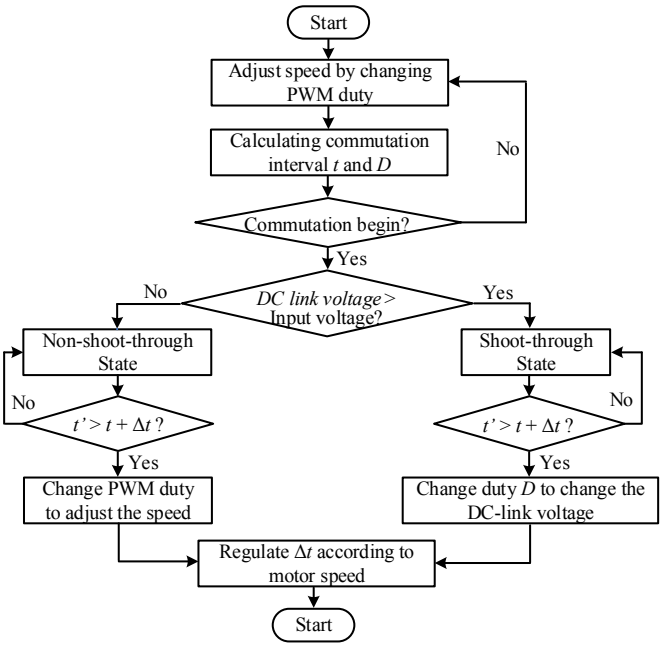


Fig. 7 Flowchart of the proposed control strategy

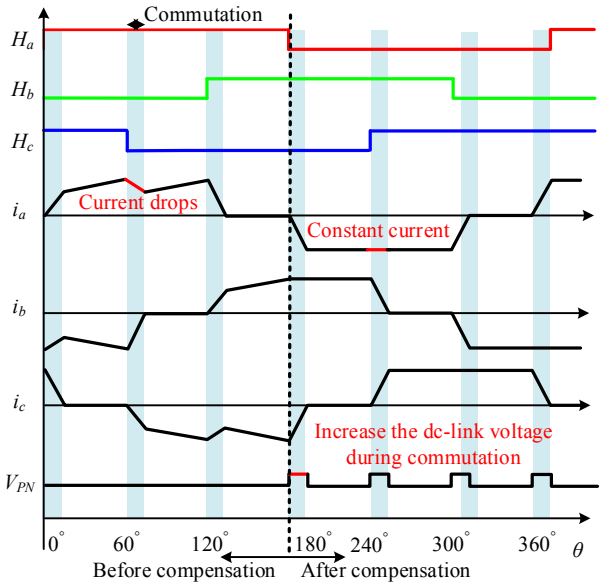


Fig. 8 Schematic diagram for reducing torque ripple

## IV. Simulation and Experiment

### A. Simulation

Matlab/Simulink model is built up and simulations are carried out to verify the effectiveness of the proposed control strategy. Parameters of the simulation system are listed as TABLE I.

Fig.9 shows the DC-link voltage and phase current of the BLDCM at the speed of 3000rpm driven by the conventional three-phase inverter. The phase current is not the rectangular wave without the compensation of the DC link voltage, since the DC-link voltage equals to the input voltage. The simulation waveform of the BLDCM driven by three-phase qZSI is shown as Fig. 10, the phase current tends to rectangular wave after increasing the DC link voltage during the commutation interval.

TABLE I
PARAMETERS OF THE BLDCM DRIVING SYSTEM

| Parameters | Values |
|---|---|
| Rated input voltage (V) | 500 |
| Rated power (kW) | 1.5 |
| Rated speed (rpm) | 3000 |
| Pole pairs | 4 |
| Phase resistance (Ω) | 2.875 |
| Phase inductance (mH) | 8.5 |

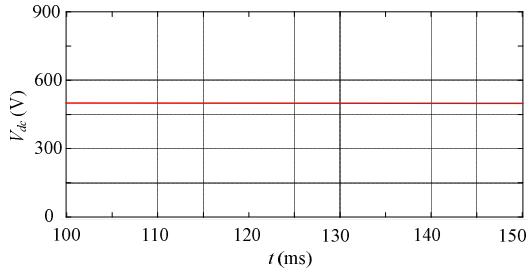


(a) DC-link voltage

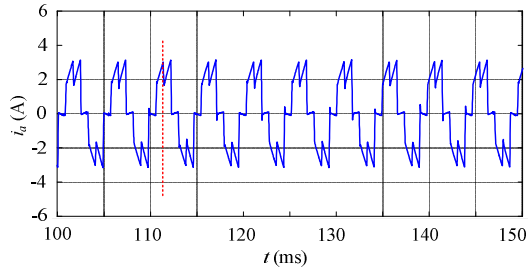


(b) Phase current

Fig. 9 Simulation results of the DC-link voltage and phase current without compensation

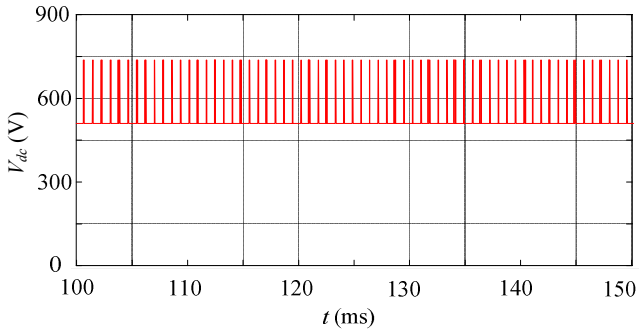


(a) DC-link voltage

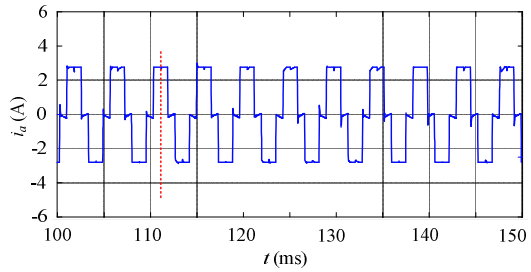


(b) Phase current

Fig. 10 Simulation results of the DC-link voltage and phase current with compensation

Fig. 11 shows the detailed DC-link voltage and three-phase current during the commutation. Fig. 12 shows the comparison of the output torque. Fig. 11 (a), (c) give the DC-link voltage and phase current before compensation, the DC-link voltage keeps constant as 500V, and the falling rate of the shutdown phase current is faster than that of opening phase current. Due to that the sum of three-phase current equals to zero, the current of non-commutation phase A decreases, and then increases to the steady value after commutation. The sag of the phase current shown as Fig. 9 (b) will result in the torque ripple, the torque ripple can be calculated from Fig. 12 (a), and the current ripple is roughly 47.6%. Fig. 11 (b), (d) give the DC-link voltage and phase current after compensation, the DC-link voltage increases to 730V, and the falling rate of the shutdown phase current is almost the same as that of the opening phase, so the non-commutation phase current basically keeps unchanged. From Fig. 10 (b), we can see that there is little depression at the top and bottom of the phase current, which is close to the ideal rectangular wave. It can be seen from Fig. 12 (b), the torque ripple is 6.2% after compensation, and the torque ripple is obviously reduced.

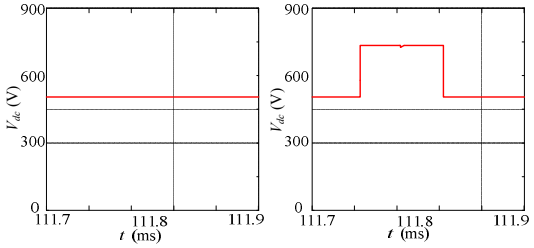


(a) DC voltage before compensation (b) DC voltage after compensation

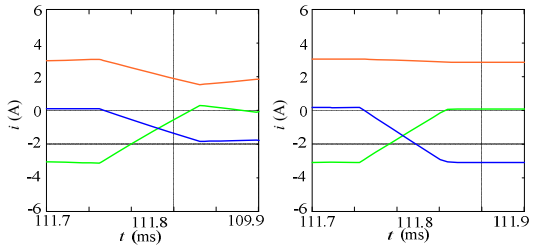


(a) Phase current before compensation (b) Phase current after compensation

Fig. 11 Details of DC link voltage and phase current during commutation

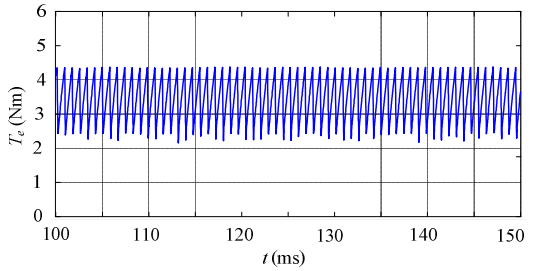


(a) Before compensation

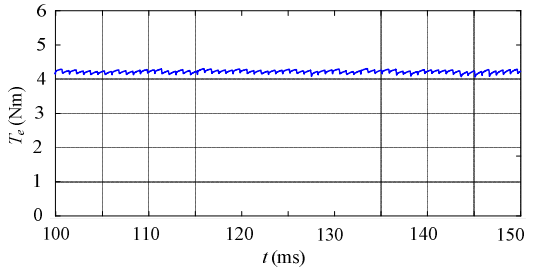


(b) After compensation

Fig. 12 Comparison of the output torque

It also can be seen from Fig. 12 that the average torque before compensation is about 3.2Nm, and it increases to 4.2Nm after compensation. Due to the increase of the DC-link voltage during the commutation and the voltage loaded to BLDCM increases, so the average torque increases.

## *B. Experiment*

The experiment is implemented on a 10W BLDCM, the DC link voltage and the phase current without and with the

impedance network are shown as Fig.13 and Fig.14. Fig.13 shows that the top of the phase current turns to more flat, and the torque ripple is reduced from 46% to below 10%. Fig. 14 shows that the slew rate of the commutation current turns to the same with the impedance network compensation.

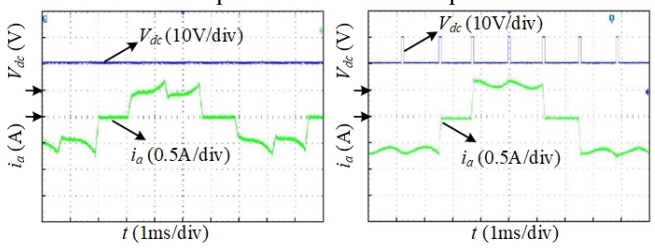


(a) Without impedance network (b) With impedance network

Fig. 13 DC link voltage and phase current

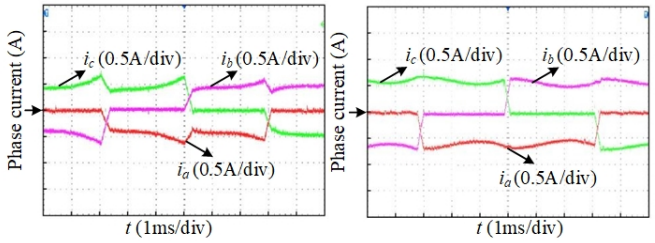


(a)Without impedance network (b) With impedance network

Fig. 14 Three phase current

## V. CONCLUSION

In this paper, the quasi-Z-source inverter is introduced and a control strategy is also proposed. This can greatly reduce the commutation torque ripple from 47.65% to 6.2%. In the method, an impedance network is placed between the power supply and the conventional three-phase inverter. In this way, the desired DC link voltage is achieved by adjusting the shoot-through duty ratio during the commutation to compensate non-commutation current. The current slew rates between shut-down phase and opening phase tend to be approximately identical, and this will dramatically reduce the commutation torque-ripple. The simulation results show that the proposed method can greatly reduce the dynamic torque ripple, and the average output torque can also be improved, leading to a good dynamic performance.

## VI. REFERENCES


[1] Y. J. Chen, B. Ruan. "Sensorless control of BLDC motor drive for a drilling rig system in shale gas development," *2016 IEEE 11th Conference on Industrial Electronics and Applications (ICIEA)*, 2016, 1508-1513.

[2] B. N. Kommula, V, R, Kota, "Performance evaluation of hybrid fuzzy PI speed controller for brushless DC motor for electric vehicle application," *2015 Conference on Power, Control, Communication and Computational Technologies for Sustainable Growth (PCCCTSG)*, Kurnool, India, Dec. 11-12, 2015, 266-270.

[3] Shakouhi, S.M., Mohamadian, M., Afjei, E.. "Torque ripple minimization control method for a four-phase brushless DC motor with non-ideal back-electromotive force," *IET Electr. Power Appl.*, 2013, vol. 7, no. 5, pp. 360–368.

[4] V. Viswanathan, J. Seenithangom, "Commutation torque ripple reduction in the BLDCM motor using modified SEPIC and three-level NPC inverter," *IEEE Transactions on Power Electronics*, 2018, vol. 33, no. 1, pp. 535-546.

[5] R. Carlson, L.-M. Milchel, and J. C. Fagundes, "Analysis of torque ripple due to phase commutation in brushless DC machines," *IEEE Transactions on Industry Applications*, 1992, vol. 28, no. 3, pp. 632-638.

[6] Y. Liu, Z. Q. Zhu, and D. Howe, "Commutation torque ripple minimizationin direct-torque-controlled PM brushless dc drives," *IEEE Trans. Ind. Electron.*, vol. 43, no. 4, pp. 1012–1021, Jul./Aug. 2007.

[7] J. E. Muralidhar; P. V. Aranasi, "Torque ripple minimization & closed loop speed control of BLDC motor with hysteresis current controller," *2014 2nd International Conference on Devices*, Circuits and Systems (ICDCS), 2014, 1-7.

[8] H. S. Hou, W. G. Liu, "Instantaneous torque ripple control in brushless DC motors based on conduction PWM duty ratio," *2015 34th Chinese Control Conference (CCC)*, 2015, pp. 4313-4318.

[9] C.L. Xia, Y. F. Wang, T. N. Shi, "Implementation of finite-state model predictive control for commutation torque ripple minimization of permanent-magnet brussless DC motor," *IEEE Transactions on Industrial Electronics*, vol. 60, no. 3, 2013, pp. 896-905.

[10] J. H. Park, Y. C. Kwak, J. W. Ahn, D. H. Lee, "A novel predicted current control scheme of BLDCMs for commutation torque ripple reduction," *2015 18th International Conference on Electrical Machines & Systems (ICEMS)*, 2015, pp. 1429-1433.

[11] W. Chen, C. L. Xia, and M. Xue, "A torque ripple suppression circuit for brushless DC motors based on power dc/dc converters," *IEEE Conference on Industrial Electronics and Applications*, 2008, pp. 1453-1457.

[12] K.Y. Nam, W.T. Lee, C. M. Lee, and J.P. Hong, "Reducing torque ripple of brushless DC motor by varying input voltage," *IEEE Transaction on Magnetics*, vol. 42, no. 4, 2006, pp. 1307-1310.

[13] F. P. Xu, T. C. Li and P. H. Tang, "A low cost drive strategy for BLDC Motor with low torque ripples," *IEEE Conference on Industrial Electronics and Applications*, 2008, pp. 2499-2502.

[14] T. N. Shi, Y. T. Guo, and S. Peng, "A new approach of minimizing commutation torque ripple for brushless DC motor based on DC-DC converter," *IEEE Transaction on Industrial Electronics*. vol. 57, No. 10, October 2010, pp. 3483-3490.

[15] B. Singh and S. Singh, "Single-phase power factor controller topology for permanent magnet brushless DC motor drives," *IET Power Electronics*. vol. 3, No. 2, 2010, pp. 147-175.


## VII. BIOGRAPHIES

**Qian Xun** was born in China, in 1990. She received B.Eng. in Automation from Hohai University, China in 2012, and M.Sc. in Power Electronics and Power Drives from Nanjing University of Aeronautics and Astronautics, China, in 2015.

After that, she had worked as a lecturer in Electrical Engineering at Huzhou University in China for 2 years, and her main research interest is permanent magnet synchronous motor control, especially for anti-disturbance control, regenerative energy storage, phase current detection for motor control and Hall rotor position estimation, and torque ripple reduction for brushless DC motor.

Since April, 2017, she has been working as a PhD student in the Division of Electrical Power Engineering at Chalmers University of Technology in Sweden. Her doctoral project is about the research on drivetrain design for fuel cell electric vehicle.

**Yujing Liu** received B.Sc., M.Sc. and Ph.D. degrees in electrical engineering from Harbin Institute of Technology, Harbin, China, in 1982, 1985, and 1988, respectively. In 1991-1994, he worked as associate professor in electromagnetic modelling and PM machine design at the same university.

In 1996-2013, he worked in ABB Corporate Research, Västerås, Sweden. In addition to develop computational tools for machine analysis and design, he has involved in investigations and studies on complex electromagnetic and thermal problems of different electrical machines, such as very high voltage machines, high-speed and high power machines, solid-pole synchronous machines, and wind generators. Between 2008 and 2013 he worked as Senior Principal Scientist in ABB group.

Since 2013, he is professor on electrical power engineering in Chalmers University of Technology. Gothenburg, Sweden. His interest includes research on motors, converters, and wireless charging for electric vehicles, generators and power electronics for tidal power conversion, and high efficiency machines for energy saving in industrial applications.

Yujing Liu is senior IEEE member and member in Swedish Standard Committee on Electrical Machines.